Available online at www.sciencedirect.com
SCIENCE DIRECT®
Journal of the European Ceramic Society 25 (2005) 99–110
www.elsevier.com/locate/jeurceramsoc

Novel polysilazanes as precursors for silicon nitride/silicon carbide composites without "free" carbon

Markus Hörz[a], Achim Zern[a], Frank Berger[b], Jörg Haug[a], Klaus Müller[b], Fritz Aldinger[a], Markus Weinmann[a,*]

[a] *Max-Planck-Institut für Metallforschung and Institut für Nichtmetallische Anorganische Materialien, Universität Stuttgart Pulvermetallurgisches Laboratorium, Heisenbergstr. 3, D-70569 Stuttgart, Germany*
[b] *Institut für Physikalische Chemie, Universität Stuttgart, Pfaffenwaldring 55, D-70569 Stuttgart, Germany*

Available online 30 September 2004

Abstract

Polysilazanes with chemical composition $Si_4N_4CH_x$ (x = 12–14) were obtained on two different reaction pathways. In the first route three equivalents of dichlorosilane, H_2SiCl_2, were mixed with one equivalent of methyldichlorosilane, $H_3CSiHCl_2$, and reacted with ammonia to yield $[(SiH_2–NH)_3(H_3CSiH–NH)]_n$ (**1**) after appropriate work-up. In the second route, dichlorosilane was reacted with methylamine and ammonia in a 3:1 ratio to deliver $[(SiH_2–NH)_3(SiH_2–NCH_3)]_n$ (**2**). The raw products were further cross-linked by base-catalyzed dehydrocoupling reactions involving Si─H and N─H units to yield products **1a** and **2a**, respectively. The molecular structure of **1** and **2** was investigated by means of high resolution ^{1}H, ^{13}C{^{1}H}, and ^{29}Si{^{1}H} NMR spectroscopy in C_6D_6 solution as well as by IR spectroscopy. Because of the insolubility of the cross-linked products **1a** and **2a** solid state ^{1}H, ^{13}C, and ^{29}Si CP-MAS NMR in combination with IR spectroscopy were applied for their spectroscopic characterization. Chemical compositions were determined using elemental analysis.

Thermolysis in an argon atmosphere up to 1400 °C of the cross-linked products delivered Si_3N_4/SiC ceramics in ∼94% yield. The absence of "free" carbon was revealed by mass spectra-coupled thermogravimetric analysis (TGA). These investigations indicated a one-step decomposition in the 250–700 °C range with predominant evaporation of hydrogen. In contrast, elimination of methane and ammonia (**1**) or methane and methylamine (**2**) was below 0.5 mass%. Additionally, neutron wide angle scattering proved the absence of a "free" carbon phase. High-temperature properties were investigated using high temperature TGA as well as XRD, EDX and TEM of annealed ceramic samples. The onset of crystallization in both materials was around 1500 and 1300 °C (1 atm N_2), respectively, and α- as well as β-Si_3N_4 formed besides α/β-SiC. Above 1900 °C ceramics derived from both **1a** and **2a** decomposed to α/β-SiC/β-Si_3N_4/α-Si composites.

Keywords: Sintering additives; Polysilylcarbodiimides; Tetrahydrofuran

1. Introduction

Silicon carbide and silicon nitride-based ceramics are refractory materials for application under severe conditions and under high stresses.[1] To overcome their low self diffusion capability their processing requires for high temperatures and the use of suitable sintering additives.[2] A main disadvantage of the sintering step is the difficulty to control the morphology of the ceramic materials under the applied conditions, i.e. the high energy input.[3]

An alternative procedure for the synthesis of silicon carbide/silicon nitride-based ceramics is the polymer-to-ceramic transformation (thermolysis) of suitable organometallic precursors,[4,5] usually oligosilazanes or polysilazanes.[6] The thermal polymer-to ceramic conversion involves a series of individual reaction steps that have to be considered carefully.[7] Nevertheless, especially precursor synthesis is a fundamental issue, since both chemical composition and molecular structure i.e. the cross-linking density of the precursors strongly influence chemical reactions that occur upon thermolysis and thus affect materials composition, structure and properties.[8]

Thermolysis is always accompanied with the formation of gaseous reaction by-products. Such species evaporate during

* Corresponding author. Tel.: +49 711 6893127; fax: +49 711 6893131.
E-mail address: weinmann@mf.mpg.de (M. Weinmann).

0955-2219/$ – see front matter © 2004 Elsevier Ltd. All rights reserved.
doi:10.1016/j.jeurceramsoc.2004.07.020

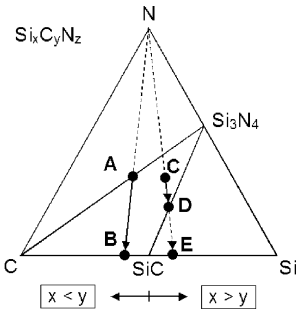

Fig. 1. Ternary Si/C/N phase diagram (T < 1484 °C, 1 bar N_2). **A**: ceramics obtained from VT50, Hoechst AG; **C**: ceramics obtained from NCP200, Nichimen Corporation, Japan. Depending on the Si:C ratio, thermal degradation of $Si_xC_yN_z$ proceeds in either one ($x < y$) or two steps ($x < y$).

the heat treatment and cause a mass loss. This mass loss along with an increase in density of the materials during thermolysis results in a significant shrinkage. Very frequently such "densification" is accompanied with formation of cracks and pores, resulting in a draw back of the specimen. As a consequence thermolysis of bulk materials under full shape retention is difficult to perform and at least requires for high ceramic yield precursors.[9]

With respect to high temperature applications it is furthermore important to consider thermodynamics of precursor-derived ceramics.[10] Silicon nitride/silicon carbide-based composites obtained from polysilazanes[2b,11–13] or polysilylcarbodiimides[14–16] usually possess chemical compositions at $Si_xC_yN_z$ ($z < 4/3x$), indicating the presence of "free" carbon. In a nitrogen atmosphere (1 atm) the thermal stability of such materials is limited. Above 1484 °C decomposition with evaporation of nitrogen takes place, because of a carbothermal reduction, i.e. reaction of "free" carbon with Si–N units according to:

$$Si_xC_yN_z \rightarrow x\mathrm{SiC} + (y - x)\mathrm{C} + \frac{z}{2}N_2$$

Fig. 1 shows a Si–C–N concentration diagram in which two polysilazane-derived materials with different composition are compared. **A**, which was obtained by thermolysis of commercially available VT 50,[17] decomposes into a SiC/C composite **B**. In contrast the Si–C–N ceramic **C** obtained from NCP200[18] under similar conditions releases a Si_3N_4/SiC composite **D**. Further heat treatment of **D** at temperatures higher than 1850 °C (1 atm N_2) causes the decomposition of silicon nitride into the elements, thus forming the SiC/Si composite **E**.[10,19] The decomposition pathway is only determined by the proportion of silicon and carbon, i.e. the share x:y. One step degradation appears if $x < y$, whereas a two step decomposition is observed if $x > y$.

It was already published that it is possible to shift the decomposition temperature of Si–C–N ceramics to higher values than 1484 °C. This requires the formation of $Si_{3+x}C_xN_4$ composites. For this purpose, excess carbon was removed by performing thermolysis in a reactive argon/ammonia atmosphere. Under such conditions, excess carbon is removed as methane (this process is frequently referred to as "carbon-burn-out").[20] For obtaining bulk ceramics however, this procedure is rather difficult to perform since it mainly affects surface-near areas.

We here describe the synthesis of polysilazanes which are designed especially to release Si_3N_4/SiC composites without free carbon, independent of the atmosphere applied during thermolysis. The intention is to design precursors in which the final elemental composition, i.e. the stoichiometry of the constituting elements of the ceramic materials is already pre-formed and which do not suffer from the release of gaseous thermolysis byproducts others than hydrogen. Therefore, the following assumptions were taken into account: Presuming exclusively hydrogen evaporation during thermolysis of poly(perhydridosilazane), $[SiH_2–NH]_n$ one would expect the formation of a silicon nitride/silicon composite, Si_3N_4 + Si. Thermolysis of poly(methylsilazane), $[H_3CSiH–NH]_n$, or poly(*N*-methylsilazane), $[SiH_2–NCH_3]_n$, under similar conditions would result in silicon nitride/silicon carbide/carbon composites, Si_3N_4 + SiC + 3C. Recently we reported in a communication[21] that co-polymers composed of (SiH_2–NH) and (H_3CSiH–NH) building blocks in a 3:1 ratio deliver Si_3N_4/SiC ceramics without "free" carbon. Here we report in detail on the synthesis, cross-linking, and thermolysis of $[(SiH_2–NH)_3(SiHCH_3–NH)]$ (**1**) and additionally present an isomer $[(SiH_2–NH)_3(SiH_2–NCH_3)]$ (**2**). The precursors only distinguish in the position of the methyl group which is either bonded to silicon (**1**) or nitrogen (**2**). Moreover, high-temperature properties i.e. thermal stability and phase evolution of the new materials by means of X-ray diffraction of annealed samples is reported.

2. Experimental

2.1. General comments

All reactions were carried out in a purified argon atmosphere using standard Schlenk techniques.[22] Tetrahydrofuran was refluxed for four days over potassium and freshly distilled prior to its use. Dichlorosilane was achieved in 99.99% purity from Sigma-Aldrich GmbH and used as-obtained. CAUTION: DICHLOROSILANE IS HIGHLY FLAMMABLE AND MAY EXPLODE WHEN GETTING IN CONTACT WITH MOISTURE OR AIR! Methyldichlorosilane was also delivered by Sigma-Aldrich and distilled from magnesium prior to its use. Ammonia and methylamine were dried over KOH. CAUTION: METHYLAMINE IS HIGHLY FLAMMABLE!

Fourier-infrared spectra were obtained with a Bruker IFS66 spectrometer in a KBr matrix. NMR experiments were performed using a Bruker Avance 250. Chemical shifts are reported in δ units (parts per million) downfield from tetramethylsilane ($\delta = 0$) with the solvent as the reference signal: ^{1}H NMR, C_6D_6 δ = 7.17; ^{13}C NMR C_6D_6 δ = 127. Solid state NMR experiments were performed on a Bruker CXP 300 or a Bruker MSL 300 spectrometer operating at a static

magnetic field of 7.05 T (^{1}H frequency: 300.13 MHz) using a 4 mm magic angle spinning (MAS) probe. ^{29}Si and ^{13}C NMR spectra were recorded at 59.60 and 75.47 MHz using the cross-polarization (CP) technique in which a spin lock field of 62.5 kHz and a contact time of 3 ms were applied. Typical recycle delays were 6–8 s. All spectra were acquired using the MAS technique with a sample rotation frequency of 5–15 kHz. ^{29}Si and ^{13}C chemical shifts were determined relative to external standard Q_8M_8, the trimethylsilylester of octameric silicate, and adamantane, respectively. These values were then expressed relative to the reference compound TMS (0 ppm). Microanalysis was performed using a combination of different equipment including Elementar Vario EL, ELTRA CS 800 C/S Determinator, LECO TC-436 N/O Determinator. Atom emission spectrometry was performed using an ISA JOBIN YVON JY70 Plus. Thermogravimetric analysis (TGA) of the polymer-to-ceramic conversion was carried out in a flowing argon atmosphere (50 cm^3/min) with a Netzsch STA 409 in alumina crucibles over a temperature of 25–1400 °C (heating rate 2 °C/min). TGA-MS was recorded at the Technische Hochschule Darmstadt in the group of Prof. Dr. Ralf Riedel using a Netzsch STA 429 thermo balance coupled with a Balzers QMA 400 cross-beam quadrupole mass spectrometer. Bulk ceramization of preceramic materials occurred in alumina Schlenk tubes in flowing argon at 25–1400 °C, heating rate 1 °C/min and a dwell time of 3 h. A Netzsch STA 501 was used for the high temperature TGA of the as-obtained ceramic samples in an argon atmosphere over a temperature range of 25–2150 °C (heating rate T < 1400 °C: 5 °C/min, T > 1400 °C: 2 °C/min) using carbon crucibles. The crystallization of as-obtained amorphous ceramics was investigated in graphite furnaces using graphite crucibles at 1300–2000 °C in 100 °C steps (heating rate T < 1400 °C: 10 °C/min, T > 1400 °C: 2 °C/min). The X-ray diffraction unit used for the structural investigations of the annealed samples was a Siemens D5000/Kristalloflex with Cu Kα_1 radiation, equipped with an OED and a quartz primary monochromator. SEM investigations were performed with a ZEISS DSM982 Gemini field emission equipment equipped with Schottky field emitter.

2.2. Polymer synthesis and characterization

2.2.1. $[(SiH_2–NH)_3(H_3CSiH–NH)]_n$ (1)

In a 2l Schlenk flask, equipped with a dry ice/isopropanol reflux condenser, a gas inlet tube and a magnetic stirrer, 35.2 g (348 mmol) of H_2SiCl_2 and 13.3 g (116 mmol) of $H_3CSiHCl_2$ were carefully dissolved in 800 ml of tetrahydrofuran which was cooled to −70 °C. Under vigorous stirring 35 g (2050 mmol) of ammonia were slowly introduced and ammonium chloride precipitation occurred immediately. The reaction mixture was then warmed to 25 °C and the ammonium chloride precipitate removed by filtration through celite. The precipitate was thoroughly extracted three times with each 100 ml of tetrahydrofuran and then disposed. After combining the filtrate and the extract and removing excess ammonia and solvent under reduced pressure at 25 °C/10^{-1} mbar, 22.3 g (115 mmol, 99% rel. to the chlorosilanes used) of $[(SiH_2–NH)_3(H_3CSiH–NH)]_n$, **1**, were obtained as a colorless liquid. For the following cross-linking step, as-obtained polymer **1** was dissolved in 200 ml of tetrahydrofuran and after adding 0.2 ml of 2.5 M *n*-BuLi in *n*-hexane (5 mmol) refluxed for ten hours. Strong gas evolution occurred thereby. At last, the solvent was removed from the mixture in high vacuum at finally 130 °C to deliver 21.5 g of precursor **1a** as a colorless coarse grained and glass-like solid.

1: IR (KBr): ν(N–H) = 3377 m; ν(C–H) = 2960 m, 2901 w, 2851 vw; ν(Si–H) = 2156 vs; δ_s(Si-CH$_3$) = 1256 m; δ(Si–N–H) = 1197 s; δ(Si–N–Si) = 897 s, br, δ(SiH$_2$) = 827 s, br cm^{-1}. ^{1}H NMR (C_6D_6): δ = 0.35 (br., SiC*H*$_3$), 0.95 (vbr., N*H*), 4.5 (br., Si*H*CN$_2$), 4.95 (br., Si*H*$_2$N$_2$). ^{13}C{^{1}H} NMR (C_6D_6): δ = −2.0, 0.8–2.2 (Si*C*H$_3$). ^{29}Si{^{1}H} NMR (C_6D_6): δ = −35.0 to −42.0 (*Si*H$_2$N$_2$), −17.0 to −22.0 (*Si*HCN$_2$). TGA (argon, 1400 °C, 74% ceramic yield): 100–800 °C, Δm = 25%; 1300–1450 °C, Δm = 1%.

1a: Anal. found: C, 6.4; H, 4.8; N, 30.1; Si, 58.7. $[CH_{14}N_4Si_4]_n$ ($[194.46]_n$). Calc.: (**1**): C, 6.18; H, 7.25; N, 28.80; Si, 57.77. IR (KBr): ν(N–H) = 3389 s; ν(C–H) = 2959 m, 2899 w; ν(Si–H) = 2154 vs; δ_s(Si–CH$_3$) = 1258 s, br; δ(Si–N–H) = 1183 s, br; δ(Si–N–Si) = 897 s, δ(SiH$_2$) = 843 s, br cm^{-1}. ^{1}H MAS NMR: δ = 1.1 (vbr., SiC*H*$_3$, N*H*), 5.4 (vbr, Si*H*). ^{13}C CP-MAS NMR: δ = 3.1 (Si*C*H$_3$). ^{29}Si CP-MAS NMR: δ = −1.7 (*Si*CN$_3$), −17.2 (*Si*CHN$_2$), −36.9 (*Si*H$_2$N$_2$). TGA (argon, 1400 °C, 94% ceramic yield): 25–200 °C, Δm = 0%; 200–1000 °C, Δm = 5.5%; 1000–1400 °C, Δm = 0.5%.

2.2.2. $[(SiH_2–NH)_3(SiH_2–NCH_3)]_n$ (2)

In a 2l Schlenk flask, equipped with a dry ice/isopropanol reflux condenser, a gas inlet tube and a magnetic stirrer, 45.6 g (452 mmol) of H_2SiCl_2 were carefully dissolved in 1000 ml of tetrahydrofuran which was cooled to −70. Under vigorous stirring 10.54 g (340 mmol) of methylamine were introduced. When the addition was finished, the mixture was warmed to 0 °C and the methylamine hydrochloride precipitate removed by filtration through an alumina filter. The precipitate was thoroughly rinsed twice with each 100 ml of ice-cold tetrahydrofuran. The combined solutions were again cooled to −70 °C and 17 g (1020 mmol) of ammonia slowly introduced. The further procedure was performed according to the synthesis of **1**. 20.3 g (104 mmol, 92% rel. to the chlorosilanes used) of **2** were obtained as a colorless liquid. The following cross-linking step was carried out according to the procedure described above for **1b**. 19.6 g of **2b** were finally obtained as a fine-grained colorless powder.

2: IR (KBr): ν(N–H) = 3450 sh, 3388 vs; ν(C–H) = 2924 m, 2852 w, 2815 vw; ν(Si–H) = 2165 vs; δ(Si–N–H) = 1157 s; δ(Si–N–Si) = 920 s, δ(SiH$_2$) 832 s cm^{-1}. ^{1}H NMR (C_6D_6): δ = 1.1 (vbr., N*H*), 2.7 (vbr., C*H*$_3$), 4.7–5.0 (vbr, Si*H*$_2$N$_2$).^{13}C{^{1}H} NMR (C_6D_6): δ = 28.9, 30.4, 31.5, 32.3 (N*C*H$_3$). ^{29}Si{^{1}H} NMR (C_6D_6): δ = −34.0 (br.). TGA

(argon, 1400 °C, 83.0% ceramic yield): 25–750 °C, Δm = 16.5%; 1200–1400 °C, Δm = 0.5%.

2a: Anal. found: C, 6.6; H, 4.5; N, 33.7; Si, 55.2. $[CH_{14}N_4Si_4]_n$ ([194.46]$_n$). Calc.: (**2**): C, 6.18; H, 7.25; N, 28.80; Si, 57.77. IR (KBr): ν(N–H) = 3406 vs; ν(C–H) = 2924 m, 2852 w, 2813 vw; ν(Si–H) = 2164 vs; δ(Si–N–H) = 1183 s; δ (Si–N–Si) = 897 s, δ (SiH_2) 843 vs cm^{-1}. ^{1}H MAS NMR: δ = 1.9 (vbr., NCH_3, NH,), 5.5 (vbr, SiH). ^{13}C CP-MAS NMR: δ = 30.1 (NCH$_3$). ^{29}Si CP-MAS NMR: δ = −36.1. TGA (argon, 1400 °C, 93.5% ceramic yield): 25–200 °C, Δm = 0.5%; 200–1000 °C, Δm = 6%; 1000–1400 °C, Δm < 0.5%.

3. Results and discussion

3.1. Synthesis

Synthesis of $[(SiH_2–NH)_3(H_3CSiH–NH)]_n$ (**1**) was performed according to:

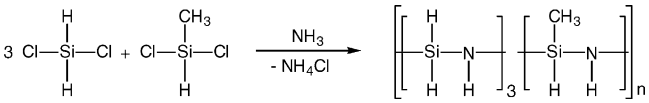

1

Dichlorosilane and methylchlorosilane were mixed in a 3:1 ratio and reacted with ammonia. Copolymer **1** was obtained by subsequent filtration and evaporation of solvent and excess ammonia under reduced pressure in 100% yield. It is a colorless low viscous liquid which is very sensitive to moisture and air. To avoid evaporation of low molecular oligomers during thermolysis, **1** was further cross-linked by a base-catalyzed dehydrogenative coupling using *n*-butyl lithium as a catalyst:

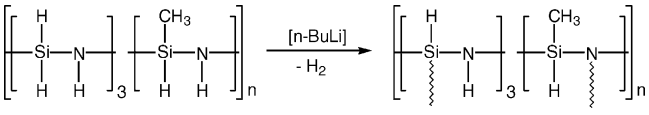

1 **1a** (schematically)

For this purpose **1** was dissolved in tetrahydrofuran and after adding 0.1 mol% of *n*-butyl lithium refluxed for 10 h. During the heat treatment, strong gas evolution and precipitation of a colorless solid was observed. After evaporation of the solvent, **1a** was isolated in 96.5 weight% as a colorless coarse-grained solid.

2 was obtained in a two step reaction. Dichlorosilane was first treated with methylamine in a 4:3 ratio and subsequently reacted with ammonia:

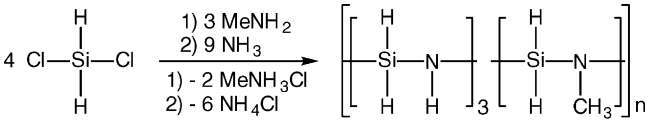

2

Methylamine hydrochloride which formed in the first reaction step was removed prior to ammonolysis. This filtration was performed to avoid trans-amination (exchange of N–H with N–CH_3 units or vice versa would change the chosen Si:C:N stoichiometry). Moreover, the reaction mixture was cooled to −70 °C during ammonolysis. After filtration, **2** was obtained as a colorless fine-grained and waxy solid in 92% yield. After further cross-linking according to the procedure applied for **1** using *n*-BuLi as a catalyst **2a** was isolated in 96.5% yield.

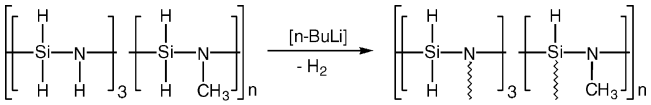

2 **2a** (schematically)

The molecular structures of all precursors were investigated by means of NMR and FT-IR spectroscopy. While the liquid polymers **1** and **2** could be investigated in C_6D_6 solution using high resolution NMR, solid state CP MAS-NMR had to be applied for the characterization of the insoluble precursors **1a** and **2a**.

3.2. Spectroscopy

3.2.1. NMR spectroscopic investigations

All NMR spectra show resonance signals in the expected chemical shift ranges. The ^{1}H NMR spectra of **1** and **2** were recorded in C_6D_6 solution. They each exhibit three sets of signals (Si–H, C–H, N–H) which possess the expected intensities. SiH protons appear as multiplets between 4.5 and 5.0 ppm. In contrast to the spectrum of **1**, in which two SiH signals at 4.5 ppm (N_2SiHMe) and 4.9 ppm (N_2SiH_2) with the expected integral intensity ratio of 1:3 are found, there is only one broad N_2SiH_2 resonance observed centered at ∼4.9 ppm in the spectrum of **2**. NH resonances in both polymers appear as broad signals at around 1 ppm. SiCH_3 protons in **1** are found at 0.35 ppm whereas those of the NCH_3 unit in **2** appear at 2.7 ppm. The different chemical environment of the methyl groups in **1** and **2** is also reflected in their ^{13}C{^{1}H} NMR spectra. They each possess a set of overlapping resonance signals: SiCH$_3$ carbon atoms in **1** are observed at ca. 0 ppm whereas NCH$_3$ carbons in **2** are found between 29 and 32 ppm. Accordingly, the ^{29}Si{^{1}H} spectrum of **1** possesses two signals centered at −37 (N_2SiH_2) and −20 ppm (N_2SiHC) whereas there is only one broad signal found in the case of **2** which is centered at −34 ppm (N_2SiH_2).

^{13}C and ^{29}Si NMR spectra of **1a** and **2a** shown in Fig. 2, which were recorded using solid state MAS with cross-polarization, are very similar to those obtained in solution.

However, it is evident that compared to the solution NMR of **1** and **2** the ^{1}H signals in the spectra obtained from the solids are significantly broadened. These ^{1}H NMR spectra do not possess any fine structure and there is consequently no detailed structural information receivable. ^{13}C CP-MAS NMR spectra show the expected resonance signals at 3 ppm (SiCH$_3$, **1a**) and 30 ppm (NCH$_3$, **2a**). During the cross-linking of **1** and **2** new Si–N units are generated at the expense of Si–H and N–H moieties. In addition to signals at −37 ppm (N_2SiH_2)

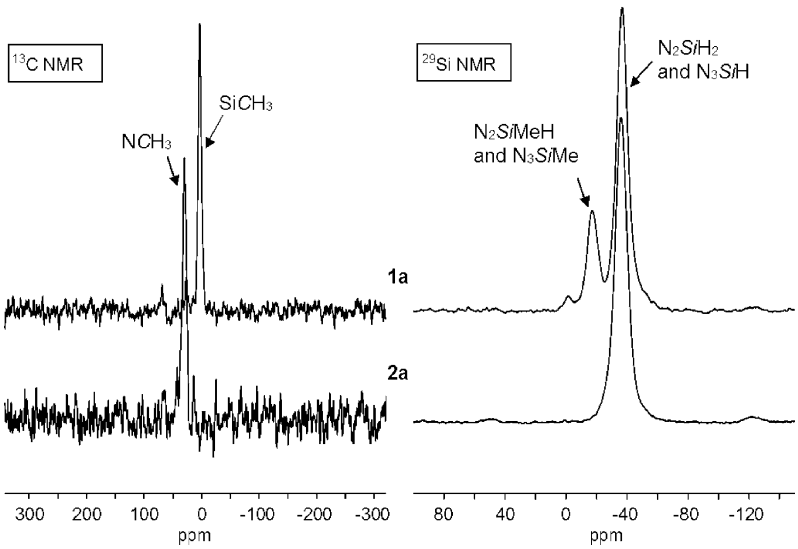

Fig. 2. ^{13}C CP-MAS NMR (75.47 MHz, left) und ^{29}Si CP-MAS NMR spectra (59.60 MHz) of the cross-linked polymers **1a** and **2a**. Sample rotation frequency 5 kHz.

and −17 ppm (N_2SiHC) in the spectrum of **1a** which were also observed for **1**, a third resonance appears at 1.7 ppm. It can be attributed to N_3SiC sites. Most probably N_3SiH sites form as well. Since the appearance of such signals is predicted at ca. −15 ppm, overlapping with N_2SiHC resonances is expected. Taking the measured ^{29}Si NMR of **2a** into account, there is surprisingly no evidence for the generation of N_3SiH sites, since only one resonance signal is observed at −36.1 ppm. This points to the fact that cross-linking either occurs to an insignificant extend or that N_2SiH_2 and N_3SiH sites have similar chemical shift ranges.

3.2.2. IR spectroscopic investigations

The IR spectra of **1**, **1a**, **2**, and **2a** each exhibit the characteristic bands of ν(N–H), ν(C–H), and ν(Si–H).[23] Additionally, very strong and broad bands referring to Si–N–H and Si–N–Si deformation vibrations are found at 1160–1200 cm^{-1} and 900–920 cm^{-1}, respectively. Deformation bands of SiH_2 units appear at 830–840 cm^{-1}. For details consider Table 1. Remarkably, the cross-linking does neither significantly influence the share of C–H:Si–H nor that of C–H:N–H even though both are expected to increase because of the consumption of N–H and Si–H during dehydrocoupling. This finding is in accordance with the conclusion received from the NMR spectra and again suggests that cross-linking takes place only to a minor extend.

Table 1
IR data (cm^{-1}) of polymers **1** and **2** and the cross-linked precursors **1a** and **2a**

	1	**1a**	**2**	**2a**
ν(N–H)	3377 (s)	3389 (s)	3450 (sh) 3388 (vs)	3406 (vs)
ν(C–H)	2960 (m) 2901 (w)	2959 (m) 2899 (w)	2922 (m) 2852 (w) 2815 (vw)	2924 (m) 2852 (w) 2813 (vw)
ν(Si–H)	2156 (vs)	2154 (vs)	2165 (vs)	2164 (vs)
δ(SiCH_3)	1256 (s, br)	1258 (s)	–	–
δ(SiNH)	1197 (s, br)	1183 (s)	1157 (s)	1188 (s)
δ(SiNSi)	897 (s, br)	897 (s)	920 (s)	897 (s)
δ(SiH_2)	827 (s, br)	843 (vs)	832 (s)	843 (vs)

3.3. Thermolysis

The thermally induced polymer-to-ceramic conversion is accompanied with the release of gaseous by-products. Their evaporation causes a mass loss and a shrinkage of the samples. The ceramic yield, which is the share of (100% × ceramic residue)/(original sample weight) strongly depends on the molecular structure, i.e. the type and structure of the polymer backbone, the degree of cross-linking and the nature of functional groups bonded to the polymer skeleton.[5,6] Such functional groups may provide latent reactivity thus enabling further thermal induced cross-linking reactions during the polymer-to-ceramic conversion. Against this incorporation of structural units that easily split of by elimination reactions such as β-hydride elimination should be avoided.

A standard method for monitoring the progress in the polymer-to ceramic conversion and for determining ceramic yields is simultaneous thermogravimetric analysis (TGA). Fig. 3 shows the results of TGA which was preformed up to 1400 °C in an argon atmosphere for as-obtained polymers **1** and **2** as well as cross-linked precursors **1a** and **2a**. As-obtained polymers **1** and **2** deliver ceramics in 77 and 83% yield, respectively. In both cases the ceramization progression is characterized by a one step decomposition beginning below 200 °C and ending between 600 and 700 °C. Additionally a mass loss of 0.5–1% is observed above 1300 °C which is most probably caused by hydrogen elimination.

In contrast to **1** and **2**, thermolysis of **1a** and **2a** is characterized by a continuous mass-loss in a one-step decomposition between 200 and 900 °C. Ceramic yields are 94 and 93.5%,

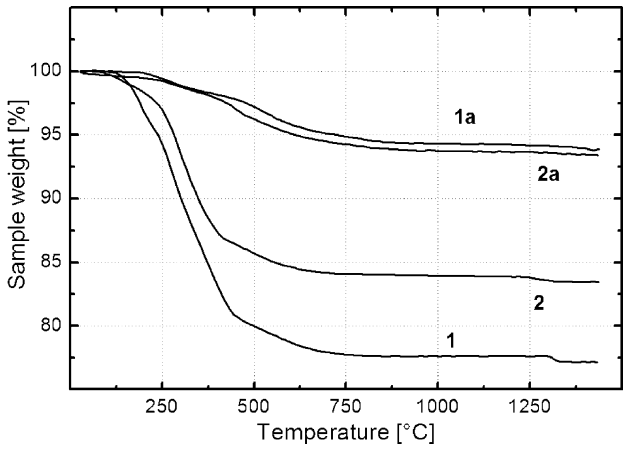

Fig. 3. Thermogravimetric analysis (TGA) of polymers **1** and **2** and cross-linked precursors **1a** and **2a**. Heating rate: 5 °C/min; atmosphere: flowing argon.

respectively. These are to our knowledge the highest ceramic yields for polymeric silazanes known so far. The remarkably high ceramic yields are a consequence of both high cross-linking density and sufficient latent reactivity of the precursor. The latter is provided by Si–H and N–H units, which enable cross-linking reactions during the heat treatment by thermally induced dehydrocoupling. The mass losses of **1a** (6%) and **2a** (6.5%) approximately correspond to their hydrogen contents determined by elemental analysis. This points to the fact that as expected exclusively hydrogen evaporates during thermolysis.

To receive reliable information on the composition of the thermolysis byproducts, additionally TGA-coupled mass spectrometry (TGA-MS) was performed. The results shown in Fig. 4 for **2a** confirm the assumption that only hydrogen is released. Results of TGA-MS of **1a** are very similar;[21] they are for this reason not discussed here.

A comparison of the relative intensities of the species with different *m*/*z* ratio clearly points to the fact that the weight loss during thermolysis is indeed predominantly caused by hydrogen (*m*/*z* = 2) evolution. Hydrogen elimination of **2a** starts at approximately 200 °C and continues up to 1000 °C. Above 1100 °C the amount of hydrogen increases again, parallel with that of a species with *m*/*z* = 18. The latter is unequivocally caused by water elimination from the surface of the alumina crucibles.

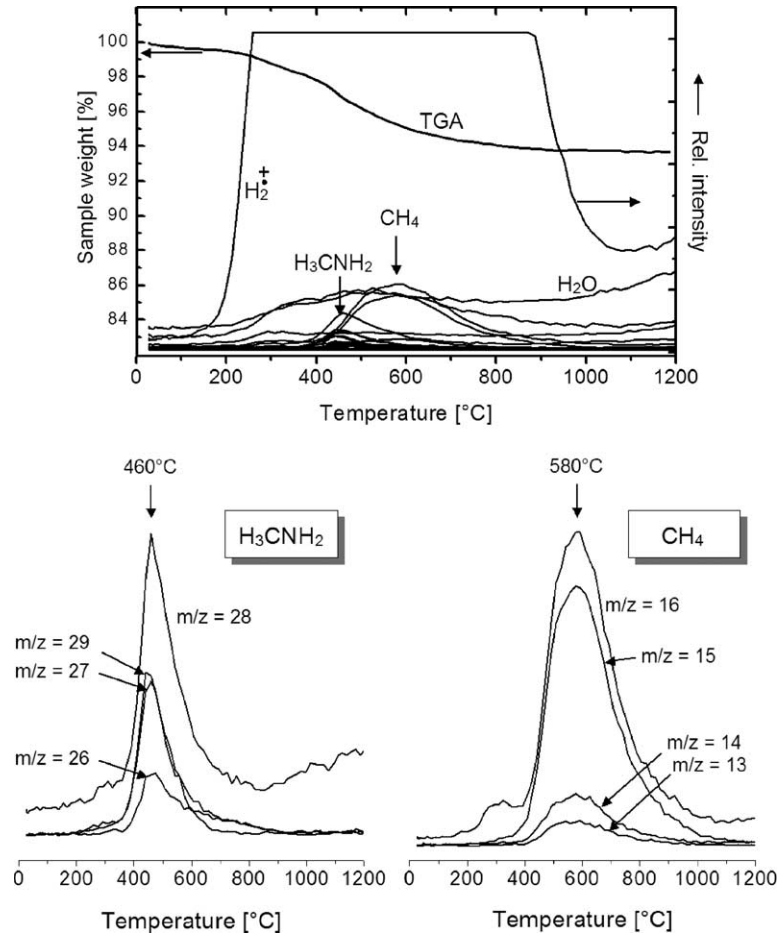

Fig. 4. TGA-MS investigations of **2a**; Top: TGA and intensities of species with *m*/*z* = 2–84. Hydrogen is the dominant gaseous thermolysis product, whereas only traces of fragments caused by methylamine (bottom left in a higher resolution) and very small amounts of methane (bottom right in a higher resolution) are detected. Heating rate: 5 °C/min; flowing argon atmosphere.

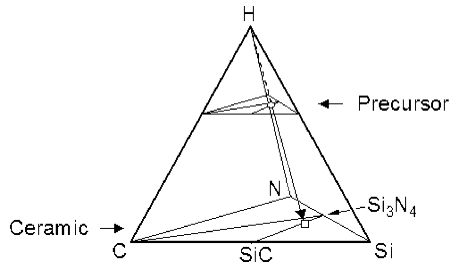

Fig. 5. Quaternary Si—C—N—H concentration diagram, representing the changes in chemical composition of **1a** and **2a** (◯) due to their transformation into ceramic materials.

The total of reaction products below 1000 °C with a higher *m*/*z* ratio than 2 is rather low. Only traces of methylamine fragments can be detected at ca. 460 °C (Fig. 4, bottom left) whereas evaporation of very small amounts of methane occurs at ca. 580 °C (Fig. 4, bottom right). A precise comparison of the relative intensities of methane and methylamine with that of hydrogen is not possible, since the large amount of hydrogen (*m*/*z* = 2) which is eliminated does not allow for a quantitative determination of cations with *m*/*z* > 2 with sufficient accuracy. An estimation of the signal intensities however suggests that the amount of methane and methylamine must be below 0.5 and 0.1 mass%, respectively. From these results it can be concluded that the Si:C:N ratio of **1a** and **2a** is retained during the polymer-to ceramic transformation as schematically pointed out in Fig. 5.

This conclusion is confirmed by a comparison of the chemical compositions of the cross-linked precursors **1a** and **2a** with those of their derived ceramics, which are given in Table 2.

3.4. Ceramic materials and high temperature investigations

Bulk ceramics were obtained by thermolysis of **1**, **1a**, **2**, and **2a** in Al_2O_3 Schlenk tubes in flowing argon gas. The precursors were therefore heated to 1200 °C using a heating rate of 1 °C/min and subsequently held for 2 h at the final temperature. Bulk ceramic yields are similar to those determined by

Table 2
Calculated and experimentally determined elemental composition (weight%) of cross-linked precursors **1a** and **2a** and ceramic materials derived thereof

			Si	N	C	H	Li
Precursor	SiCNH[a]	calc.	57.8	28.8	6.2	7.2	0
	1a	det.	58.7	30.1	6.4	4.8	n.d.[c]
	2a	det.	55.2	33.7	6.6	4.5	n.d.[c]
Ceramic	Si_4N_4C[b]	calc.	62.2	31.1	6.7	0	0
	1a	det.	60.5	33.6	5.9	<0.1	n.d.[c]
	2a	det.	60.7	35.0	4.3	<0.1	n.d.[c]

[a] Calculated for $[(H_2Si\text{-}NH)_3(HSi(CH_3)\text{-}NH)]_n$ or $[(H_2Si\text{-}NH)_3(H_2Si\text{-}N(CH_3))]_n$.
[b] Calculated for $Si_3N_4{\cdot}SiC$.
[c] Not detectable.

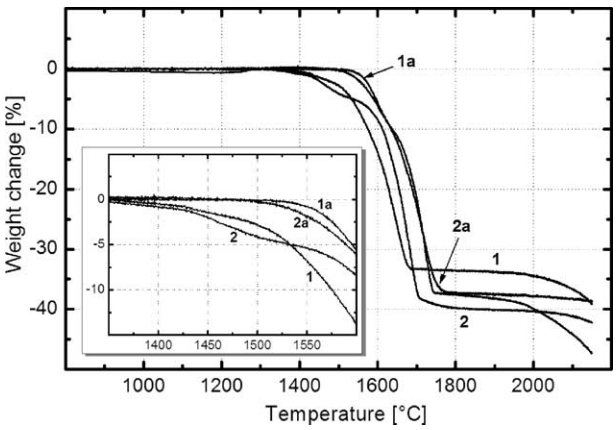

Fig. 6. High temperature TGA of ceramics derived from polymers **1**, **2** and cross-linked precursors **1a** and **2a**; Heating rate T < 1400 °C: 5 °C/min, T > 1400 °C: 2 °C/min; Argon atmosphere. The insert gives the temperature range 1350–1600 °C in a higher magnification.

TGA. Ceramics obtained from polymers **1** and **2** are brown glass-like materials whereas ceramics derived from cross-linked precursors **1a** and **2a** are gray substances. Chemical compositions of the precursors and the ceramic materials are given in Table 2.

High-temperature properties were investigated using high temperature TGA in Argon up to 2150 °C (Fig. 6) and X-ray diffraction of ceramic samples that were annealed at temperatures between 1300 and 2000 °C (Figs. 7, 8 and 12).

Fig. 6 demonstrates that ceramics derived from cross-linked precursors **1a** and **2a** possess – even though obtained from structurally different polymers – nearly identical high

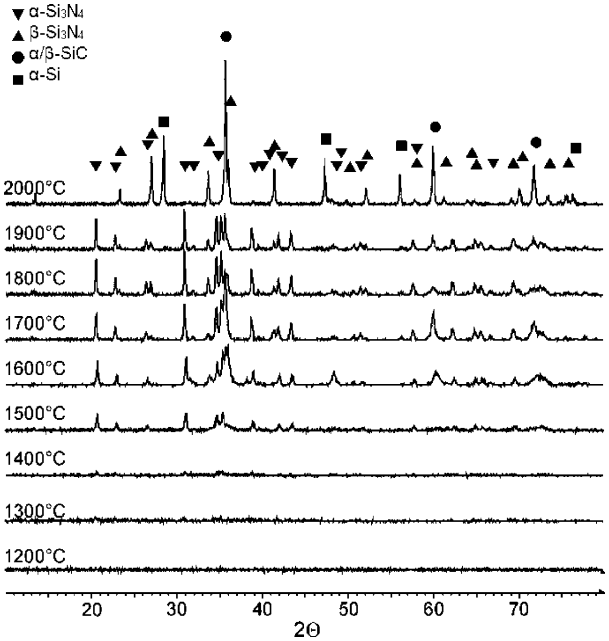

Fig. 7. X-ray powder diffraction patterns of ceramics obtained from cross-linked precursor **1a** after thermolysis at 1200 and annealing at 1300–2000 °C (100 °C steps) in 1 bar nitrogen for 3 h.

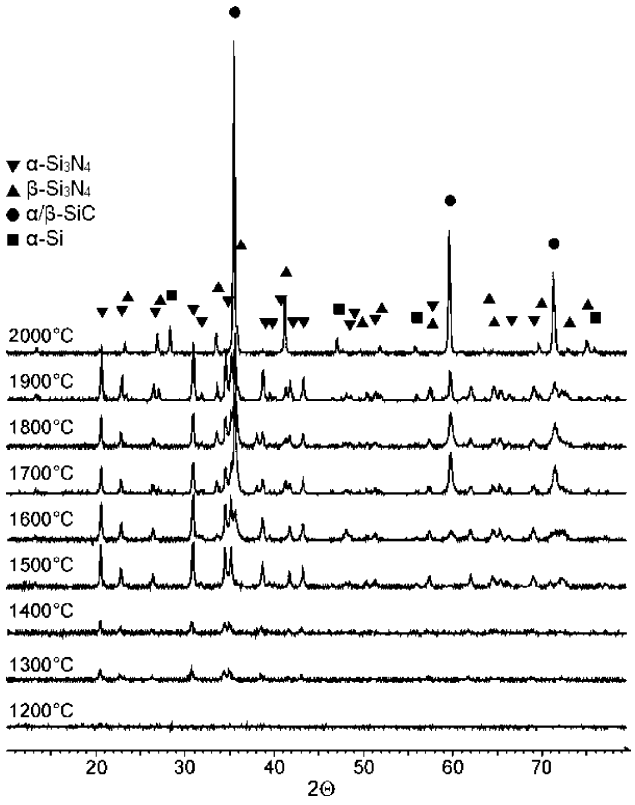

Fig. 8. X-ray powder diffraction patterns of ceramics obtained from cross-linked precursor **2a** after thermolysis at 1200 and annealing at 1300–2000 °C (100 °C steps) in 1 bar nitrogen for 3 h.

temperature mass stability. They decompose in a one-step reaction. The onset of decomposition is at 1520 °C for **2a** ceramics and at 1540 °C for **1a** ceramics. The mass loss which is ∼35% at 1800 °C corresponds to the nitrogen content of the materials determined by elemental analysis (Table 2) and points to a quantitative degradation of Si–N units. These values are slightly higher than those observed for Si–C–N ceramics which contain "free" carbon. The unexpected additional degradation step of **1a** above 1900 °C is not yet understood. Ceramics derived from polymers **1** and **2** behave different. Degradation already begins at 1350 °C and mass losses are 33% (**1**) and 40% (**2**). This observation indicates that the cross-linking step performed prior to the polymer-to-ceramic conversion (**1a**, **2a**) does not only increase ceramic yields. It also directly enhances high-temperature properties of the precursor-derived ceramics.

The heat treatment of the materials is accompanied with the formation of crystalline phases. Phase evolution in general is a function of the elemental composition, annealing temperature, annealing time and applied atmosphere. In this study however, only the annealing temperature was varied.

Ceramics were annealed as-obtained after thermolysis in a nitrogen atmosphere at temperatures between 1300 and 2000 °C using a heating rate of 10 °C/min below 1200 °C and 2 °C/min above 1200 °C. The samples were held for 3 h at the final annealing temperature and after cooling to room temperature homogenized by milling in a tungsten carbide ball mill. The particle size after ball milling was below 32 μm. X-ray powder diffraction was performed in the 2θ range 10°–80°. Results are shown in Fig. 7 (**1a** ceramics) and Fig. 8 (**2a** ceramics).

Ceramics received from **1a** and **2a** possess a very similar crystallization behavior. Though after annealing at higher temperatures complex diffraction patterns are obtained, all reflections can be assigned unequivocally.

As-obtained **1a** and **2a** ceramics are fully amorphous. Even after heating to 1400 °C no reflections in the X-ray pattern of **1a** are found that might indicate crystallization. Nevertheless, investigations by means of neutron small angle scattering (Fig. 9) clearly display a near-range order, even if thermolysis is performed at lower temperature, for example 1050 °C.

A comparison of total structure factors $S(q)$ (Fig. 9, top) and the pair correlation functions $G(r)$ (Fig. 9, bottom) of **1a** ceramics with those of amorphous carbon and amorphous

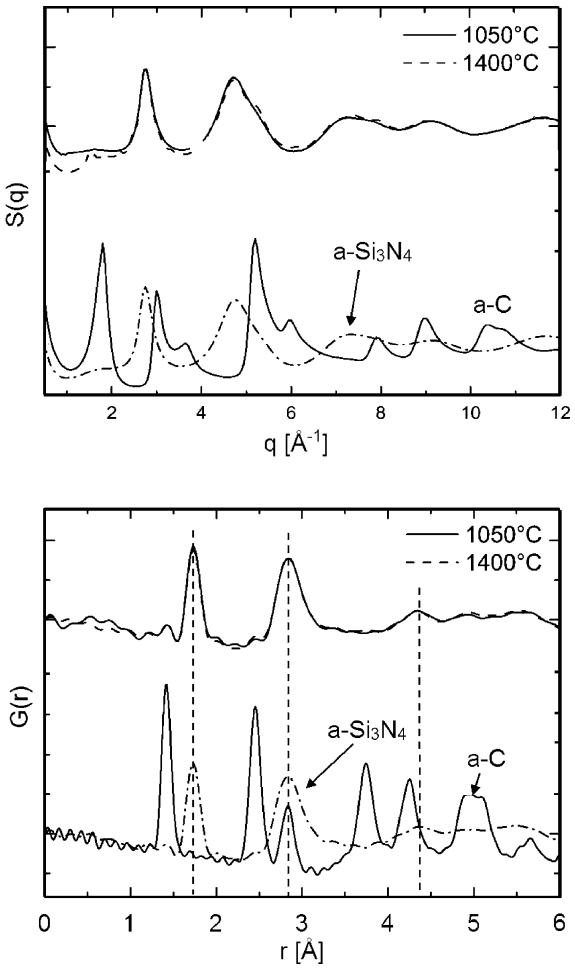

Fig. 9. Total structure factors $S(q)$ (top) and pair correlation functions $G(r)$ (bottom) obtained by neutron diffraction experiments of **1a** ceramics after thermolysis at 1050 °C and annealing at 1400 °C (16 h) in a nitrogen atmosphere. Structure factors and pair correlation functions of amorphous carbon and amorphous silicon nitride are provided for a comparison.

silicon nitride indicate that silicon nitride segregation already appears during thermolysis. Since furthermore as-obtained and annealed ceramics possess almost identical diffraction patterns one can conclude that annealing at 1400 °C does not significantly influence the structural evolution of the material. The most important aspect however is the lack of neutron reflections displaying "free" (sp^2) carbon segregation which is always observed in Si_3N_4/C or SiC/Si_3N_4/C composites.

Increasing the annealing temperature of **1a** ceramics to 1500 °C (Fig. 7) results in the appearance of a set of reflections which indicate the onset of phase separation, i.e. crystallization of α-Si_3N_4. These reflections increase in intensity after heating to 1600 °C. Moreover, additional reflections become visible which can be attributed to β-Si_3N_4 and SiC. An unambiguous assignment of the silicon carbide modification however is not possible, since the reflections superimpose with those of the more intensive silicon nitride reflections.

Further increasing the annealing temperature to 1800 °C does not cause major changes in the phase composition of **1a** ceramics. Crystalline phases assigned from X-ray powder diffraction are α- and β-Si_3N_4 as well as SiC.

The appearance of "free" carbon can also be excluded considering energy-filtered TEM investigations (EF TEM). Fig. 10 displays the results of these investigations for **1a** ceramics annealed at 1800 °C.

The bright field image in Fig. 10 (top, left) indicates that the specimen after annealing at 1800 °C is composed of crystal grains with sizes ranging up to ca. 500 nm. There is no evidence for a third phase in between the individual grains,

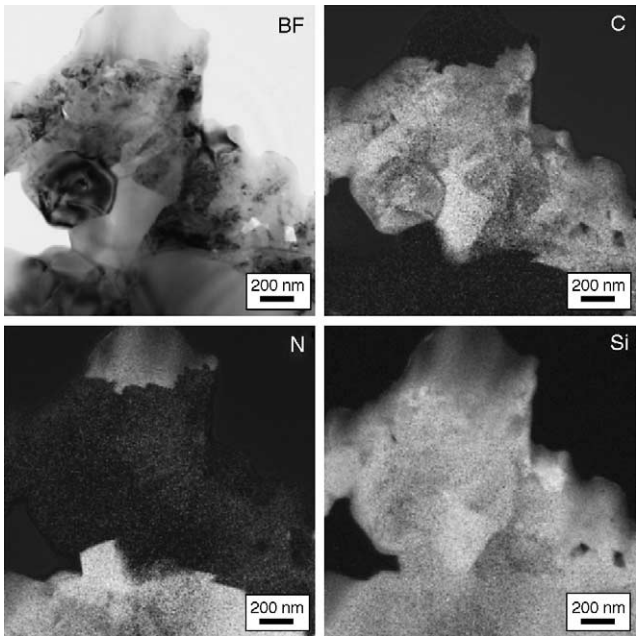

Fig. 10. Energy-filtered TEM investigations (EF TEM) of **1a** ceramics after annealing at 1800 °C (3 h, 1 bar N_2 atmosphere). Upper left: bright field image. Upper right and bottom: carbon, nitrogen and silicon distribution. Nano-sized silicon carbide and silicon nitride are visible, whereas there is no indication for carbon or silicon segregation.

which are directly attached to each other. The silicon map displays homogeneous distribution of silicon throughout the sample. Carbon-containing areas are free of nitrogen and vice versa. Consequently, the material is composed of silicon carbide and silicon nitride crystals, which is in accordance with the findings obtained by X-ray diffraction (Fig. 7). The average diameter of SiC crystals is between 100 and 400 nm whereas that of Si_3N_4 crystals is between 300 and 500 nm.

Further increasing the annealing temperature to 1900 °C again has no major influence on the phase evolution. Both position and intensity of the individual reflections remain similar even though thermodynamics predict decomposition of silicon nitride into the elements.

Such degradation however takes place when heating the sample to 2000 °C. New reflections at 28.4°, 47.2° and 56.0° which correspond to α-silicon become visible. Moreover, α-Si_3N_4 reflections vanish completely and the intensity of β-Si_3N_4 reflections decreases significantly. In contrast, reflections corresponding to silicon carbide sharpen and increase in intensity. The observation of β-Si_3N_4 reflections is most probably a consequence of silicon nitridation during the cooling of the sample (see below).[24]

Remarkably, **1a** and **2a** derived ceramics distinguish in their crystallization behavior at low temperature. In contrast to **1a** ceramics, there are reflections already observed in the X-ray patterns of **2a** ceramics after annealing at 1300 °C (Fig. 8) which point to a considerable amount of crystalline phases. The pattern is almost identical with that of **1a** ceramics after annealing at 1500 °C; the detected reflections correspond to α-Si_3N_4. The earlier crystallization of **2a** ceramics is most probably a consequence of a de-mixing already during thermolysis. Laine et al.[25] in 1995 compared thermolysis of methyl-substituted polysilazanes of the general type $[Si(R)(CH_3)–NH]_n$ (**A**) and $[Si(R)H–N(CH_3)]_n$ (**B**). They found that the structure of the derived ceramics strongly depends on the position of the methyl groups within the polymer framework. Whereas the carbon atoms of the methyl groups in **A** remained on silicon, thus forming ceramics with $Si(C,N)_4$ structural units, carbon atoms of methyl groups bonded to nitrogen segregated as "free" sp^2 carbon. These studies give clear hints to understand the earlier crystallization of silicon nitride in **2a** ceramics. During thermolysis, Si–N bonds are generated by dehydrocoupling of Si–H and N–H units already at moderate temperature, whereas dehydrocoupling of C–H and Si–H with formation of Si–C bonds takes place at considerable higher temperature. The main difference in the polymer structure of **1a** and **2a** is that the first exhibits silicon bonded in Si–N and Si–C units, whereas **2a** is exclusively composed of Si–N motifs. For this reason extended areas with silicon in SiN_4 environments can form during the heat treatment of **2a** already at comparably low temperature. These areas can be regarded as segregations of amorphous silicon nitride, which crystallize earlier than ternary Si–C–N composites. SiN_3C sites present in **1a** ceramics, in contrast obviously inhibit early crystallization of silicon nitride efficiently. Exceeding 1600 °C, the differences

vanish. This points to the fact that the phase evolution at and above this temperature is determined exclusively by the composition of the samples (which is similar) and not by the molecular structure of the polymeric precursors.

Scanning electron microscopic (SEM) investigations of surface areas of annealed **1a** bulk ceramics mirror the findings obtained from X-ray diffraction of ceramic powders. Bulk materials required for this purpose were obtained by warm uniaxial pressing of the precursor powder at 280 °C/45 MPa and subsequent thermolysis (1200 °C, 3 h, argon). Fig. 11 displays the result of such a surface investigation of **1a** ceramics after annealing at 2000 °C. The area displayed represents the typical structure throughout the sample.

The specimen has a crack-free surface which is covered with rods and whiskers. Pores are present only to a minor extend. The determination of the chemical composition was performed by energy-disperse X-ray diffraction (EDX). Crosses in the images indicate investigated spots. It is found that the surface is composed exclusively of silicon and silicon carbide. In contrast, nitrogen-containing segregation is not observed. Images (b) and (c) exhibit areas containing rods (b) and whiskers (c) in a higher magnification. Rods with an average diameter of 5–10 μm and lengths up to 200 μm as well as whiskers with similar lengths but smaller diameter (<2 μm) are each composed of silicon nitride. The appearance of silicon nitride with such "uniaxial" shape points to the fact that its growth appeared by gas phase reactions, i.e. nitridation of elemental silicon during the cooling of the specimen after annealing.[24] Consequently silicon nitride formation is limited to surface areas. EDX investigations of the interior of the sample (not shown) clearly display a totally different situation. In this region only silicon and carbon are determined whereas there is no indication for nitrogen containing phases.

This is also reflected by X-ray diffraction experiments shown in Fig. 12 of the sample interior.

From 1700–1900 °C the X-ray diffraction patterns, i.e. position and intensity of the individual reflections of **1a** ceramic powders and the interior of ceramic bulk material are almost similar. One observes α-Si_3N_4, β-Si_3N_4, as well as SiC reflections but no reflections indicating silicon segregation. After annealing at 2000 °C however, the situation changes. While in the X-ray pattern of ceramic powders (Fig. 7) intensive reflections of β-Si_3N_4, α/β-SiC, and α-Si are visible, α/β-SiC and α-Si are the only crystalline phases detected within the bulk sample. These findings suggest, that the phase evolution of the materials during/after annealing at 2000 °C proceeds diffusion-controlled. Above 1900 °C both α-Si_3N_4 and β-Si_3N_4 dissociate into the elements. Because

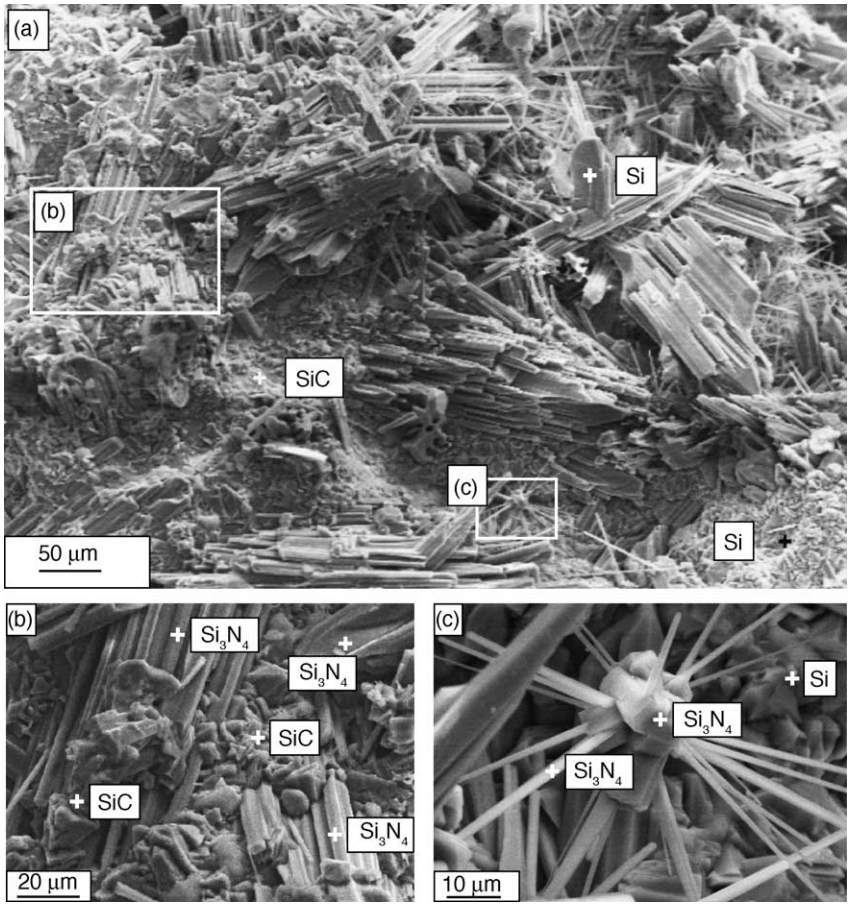

Fig. 11. SEM micrographs of the surface area of **1a** ceramics after annealing at 2000 °C under nitrogen gas. (a) 200× magnification; clip (b) 2000× magnification; clip (c) 1000× magnification. Spots investigated using energy-disperse X-ray diffraction (EDX) are marked by a cross.

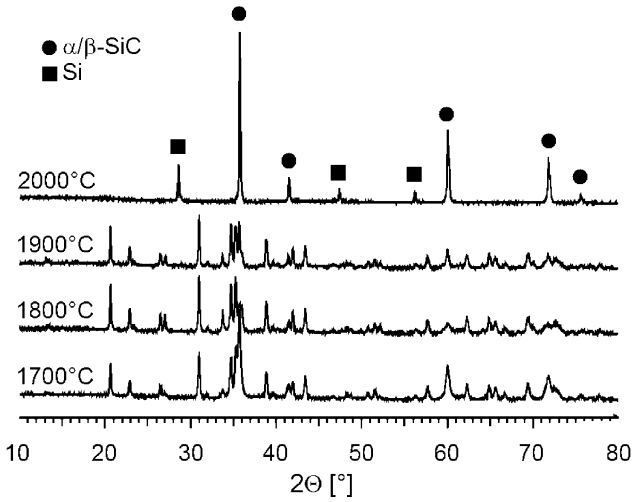

Fig. 12. X-ray powder diffraction patterns of the interior of bulk ceramics obtained from cross-linked precursor **1a** after annealing at 1700–2000 °C (100 °C steps) in 1 bar nitrogen for 3 h. In contrast to **1a** powders (cf. Fig. 7) there is no evidence for silicon nitride formation after annealing at 2000 °C.

of the long annealing time, nitrogen which forms completely escapes from the sample. During cooling, the back reaction takes place. Since cooling proceeds rather fast, there is only restricted diffusion of nitrogen from the environment into the sample, thus limiting silicon nitride formation to the sample surface.

4. Conclusions and outlook

The preparation of precursor-derived Si–C–N ceramics without "free" carbon can be realized by synthesizing polymers which possess the desired Si:C:N ratio of the final ceramics and which release hydrogen as the only gaseous reaction product during the polymer-to-ceramic conversion. For example, Si_3N_4/SiC composites (Si_4N_4C) can be obtained from two structurally different polysilazanes, $[(SiH_2–NH)_3(H_3CSiH–NH)]_n$ (**1**) and $[(SiH_2–NH)_3(SiH_2–NCH_3)]_n$ (**2**). To avoid depolymerization and/or volatilization of low-weight molecular components during thermolysis additional cross-linking is required. The cross-linked precursors deliver ceramics in ca. 95% yield and hydrogen is the only gaseous reaction product. High-temperature properties i.e. mass stability and crystallization/decomposition only depend on the overall composition. Above 1500 °C, α-Si_3N_4, β-Si_3N_4, and SiC segregate. Such compositions are stable up to 1900 °C. At 2000 °C α-Si_3N_4 and β-Si_3N_4 dissociate into the elements. During cooling, back reaction, i.e. nitradation of silicon with formation of β-Si_3N_4 takes place in surface-near areas. Degradation by a carbothermal reaction as observed for carbon-containing composites is not observed. Crystallization below 1500 °C is influenced strongly by the polymer structure. It is found that Si–C units in the polymer backbone inhibit silicon nitride crystallization. For this reason we are currently investigating the synthesis of Si_3N_4/SiC composites with higher amounts of SiC. Two possible approaches which were already performed successfully and which will be published soon are (i) replacement of the SiC unit ($H_3CSiH–NH$) in **1** with $(SiH_2C_2H_4SiH_2)_2–NH$) building blocks and cross-linking of **1** or **2** in the presence of $H_3SiC_2H_4SiH_3$. While the first approach releases $Si_3N_4{\cdot}2SiC$ the latter allows for producing Si_3N_4/SiC composites with even higher SiC contents.

Acknowledgements

The authors greatly acknowledge Martina Thomas for her assistance in recording XRD spectra, Gerhard Kaiser for performing elemental analysis, Hartmut Labizke for his help in the SEM investigations and Horst Kummer for recording high temperature TGA. Thanks also to Prof. Dr. Ralf Riedel and Claudia Fasel (Technische Universität Darmstadt, Germany) for performing TGA MS investigations. This work was financially supported by the Deutsche Forschungsgemeinschaft (DFG).

References

1. Evans, A. G., In *High-Temperature Structural Materials*, ed. R. W. Cahn, A. G. Evans and M. McLean. Chapman & Hall, London, 1996.
2. (a) *Silicon Nitride-Based Ceramics*, ed. M. J. Hoffmann, P. F. Becher and G. Petzow. Trans Tech. Publications, Aedermanndorf, 1994;
   (b) Silicon nitride ceramics: scientific and technological advances. In *Mater. Res. Soc. Symp. Proc.*, ed. I.-W. Chen, P. F. Becher, M. Mitomo, G. Petzow and T.-S. Yen. 1993, p. 287;
   (c) Mitomo, M. and Petzow, G., *Mater. Res. Soc. Bull.*, 1995, **20**, 19.
3. Lange, F. F., *J. Am. Ceram. Soc.*, 1979, **62**, 428.
4. (a) Zeldin, M., Wynne, K. J. and Allcock, H. R., ed., *Inorganic and Organometallic Polymers, Advanced Materials and Intermediates, ACS Symposium Series 360*. American Chemical Society, Washington, DC, 1988;
   (b) Peuckert, M., Vaahs, T. and Brück, M., *Adv. Mater.*, 1990, **2**, 398;
   (c) Toreki, W., *Polym. News*, 1991, **16**, 1;
   (d) Wisian-Neilson, P., Allcock, H. R. and Wynne, K. J., ed., *Inorganic and Organometallic Polymers II, Advanced Materials and Intermediates, ACS Symposium Series 572*. American Chemical Society, Washington, DC, 1994;
   (e) Birot, M., Pillot, J.-P. and Dunogués, J., *Chem. Rev.*, 1995, **95**, 1443.
5. (a) Weinmann, M., Aldinger, F. *et al.*, In *The Handbook of Advanced Materials*, ed. M. Somiya. Elsevier, 2003, p. 265;
   (b) Materials science and technology, In *Advanced Ceramics from Inorganic Polymers*, ed. R. Riedel, R. W. Cahn, P. Haasen and E. J. Kramer. VCH, Weinheim, 1996, p. 1 (chapter 11).
6. (a) For recent reviews on organic silicon compounds as precursors for ceramics see Laine, R. M. and Sellinger, A., Si-containing ceramic precursors. In *The Chemistry of Organic Silicon Compounds*, ed. Z. Rappoport and Y. Apeloig. John Wiley & Sons, London, 1998, p. 2;
   (b) Kroke, E., Li, Y.-L., Konetschny, C., Lecomte, E., Fasel, C. and Riedel, R., *Mater. Sci. Eng.*, 2000, **R26**, 97.
7. (a) Laine, R. M. and Babonneau, F., *Chem. Mater.*, 1993, **5**, 260;
   (b) Schuhmacher, J., Weinmann, M., Bill, J., Aldinger, F. and Müller, K., *Chem. Mater.*, 1998, **10**, 3913;

(c) Schuhmacher, J., Berger, F., Weinmann, M., Bill, J., Aldinger, F. and Müller, K., *Appl. Organomet. Chem.*, 2001, **15**, 809;
(d) *Proc. Werkstoffwoche 1998. Band VII, Keramik/Simulation*, ed. J. Schuhmacher, K. Müller, M. Weinmann, J. Bill and F. Aldinger. In: Heinrich J, Ziegler G, Hermel W, Riedel H. Wiley-VCH, Weinheim, 1999, p. 321.

8. Weinmann, M., Habilitation thesis, Universität Stuttgart, Germany, 2003.
9. (a) Riedel, R., Pasing, G., Schönfelder, H. and Brook, R. J., *Nature*, 1992, **355**, 714;
(b) Riedel, R., Seher, M., Mayer, J. and Szabó, D.-V., *J. Eur. Ceram. Soc.*, 1995, **15**, 703;
(c) Haug, R., Weinmann, M., Bill, J. and Aldinger, F., *J. Eur. Ceram. Soc.*, 1999, **19**, 1;
(d) Seitz, J. and Bill, J., *J. Mater. Sci. Lett.*, 1996, **15**, 391.
10. (a) Seifert, H. J. and Aldinger, F., *Z. Metallkd.*, 1996, **87**, 841;
(b) Seifert, H. J. and Aldinger, F., In *Precursor-Derived Ceramics*, ed. J. Bill, F. Wakai and F. Aldinger. Wiley-VCH, Weinheim, 1999, p. 165;
(c) Seifert, H. J., Lukas, H.-L. and Aldinger, F., *Ber. Bunsenges. Phys. Chem.*, 1998, **102**, 1309;
(d) Seifert, H. J. and Aldinger, F., *Struct. Bonding*, 2002, **101**, 1.
11. (a) Chantrell, P. G. and Popper, P., *Special Ceramics 1964* For recent reviews on organic silicon compounds as precursors for ceramics see. Academic Press, London, New York, 1965;
(b) Popper, P., *Br. Ceram. Res. Assoc. Spec. Publ.*, 1967, **57**, 1.
12. (a) Lavedrine, A., Bahloul, D., Goursat, P., Choong Kwet Yive, N. S., Corriu, R. J. P., Leclercq, D. *et al.*, *J. Eur. Ceram. Soc.*, 1991, **8**, 221;
(b) Choong Kwet Yive, N. S., Corriu, R. J. P., Leclercq, D., Mutin, P. H. and Vioux, A., *New J. Chem.*, 1991, **15**, 85;
(c) Choong Kwet Yive, N. S., Corriu, R. J. P., Leclercq, D., Mutin, P. H. and Vioux, A., *Chem. Mater.*, 1992, **4**, 141;
(d) Bahloul, D., Pereira, M., Goursat, P., Choong Kwet Yive, N. S. and Corriu, R. J. P., *J. Am. Ceram. Soc.*, 1993, **76**, 1156.
13. Vaahs, T., Brück, M. and Böcker, W. D. G., *Adv. Mater.*, 1992, **4**, 224.
14. (a) Ebsworth, E. A. and Mays, M. J., *J. Chem. Soc.*, 1961, 4879;
(b) Ebsworth, E. A. and Mays, M. J., *Angew. Chem.*, 1962, **74**, 117.
15. (a) Pump, J. and Wannagat, U., *Angew. Chem.*, 1962, **74**, 117;
(b) Pump, J. and Wannagat, U., *Ann. Chem.*, 1962, **652**, 21.
16. (a) Kienzle, A., Obermeyer, A., Riedel, R., Aldinger, F. and Simon, A., *Chem. Ber.*, 1993, **126**, 2569;
(b) Gabriel, A. O. and Riedel, R., *Angew. Chem. Int. Ed. Engl.*, 1997, **36**, 384;
(c) Gabriel, A. O., Riedel, R., Storck, S. and Maier, W. F., *Appl. Organomet. Chem.*, 1997, **11**, 833;
(d) Riedel, R. and Gabriel, A. O., *Adv. Mater.*, 1999, **11**, 207.
17. VT50 was a commercially available polyvinylsilazane of Hoechtst AG (Germany).
18. NCP200 is a commercially available polyhydridomethylsilazane of Nichimen Inc. (Chisso, Japan).
19. (a) Peng, J., Ph.D. thesis, Universität Stuttgart, Germany, 2002;
(b) Seifert, H. J., Habilitation thesis, Universität Stuttgart, Germany, 2003.
20. Galusek, D., Reschke, S., Riedel, R., Dreβler, W., Šajgalik, P., Lenčéš, Z. *et al.*, *J. Eur. Ceram. Soc.*, 1999, **19**, 1911.
21. Weinmann, M., Zern, A. and Aldinger, F., *Adv. Mater.*, 2001, **13**, 1704.
22. This preparative method is based on experiments developed by the German chemist Wilhelm Schlenk. All apparatus are equipped with sidearms for pumping out the air and moisture and introducing inert gas. See also: Shriver, D. F. and Drezdzon, M. A, *The Manipulation of Air-Sensitive Compounds* (*2nd ed.*). Wiley, New York, 1986.
23. Socrates, G., *Infrared Characteristic Group Frequencies*. John Wiley & Sons Ltd., West Sussex, 1994.
24. Messier, D. R. and Wang, P., *J. Am. Ceram. Soc.*, 1973, **56**, 480.
25. (a) Laine, R. M., Babonneau, F., Blowhowiak, K. Y., Kennish, R. A., Rahn, J. A., Exarhos, G. J. *et al.*, *J. Am. Ceram. Soc.*, 1995, **78**, 137;
(b) Blum, Y. D., Schwartz, K. B. and Laine, R. M., *J. Mater. Sci.*, 1989, **24**, 1707.